DSS-14 Subreflector Actuator Dynamics During the Landers Earthquake

R. Levy and D. Strain
Ground Antennas and Facilities Engineering Section

The June 28, 1992, Landers earthquake ground motion records at the Echo site (DSS-12 antenna) were adjusted to provide a better match with spectra from the measured Mars site (DSS-14 antenna) instrument tower response. A finite-element model of the antenna structural system was analyzed for response to this ground motion. Dynamic forces and displacements were computed in the locality of components that had failed during the earthquake. Calculated forces in the range of from 30,000 to 35,000 lb on failed Y-axis actuator U-joints were consistent with laboratory load tests. The load capacity of these joints was found to be below the range of from 34,000 to 42,000 lb. Dynamic amplification factors of from 6 to 16 were computed for the quadripod apex accelerations with respect to the ground accelerations. The largest amplification factor—25—was found at the outboard end of the X-actuator.

I. Introduction

The June 28, 1992, Landers earthquake shock arrived at the JPL Goldstone Complex at about 5 a.m. PDT, causing failures within components of the Mars antenna subreflector positioner assembly and damage to the subreflector. The antenna is shown in Fig. 1 at a 15-deg elevation, which was the attitude at the time of the earthquake. The epicenter was about 55 kilometers to the southeast of the antenna complex, and the main shock, of magnitude 7.4, occurred at the Camp Rock–Emerson Fault and its southern extension. Strong aftershocks occurred within several hours, but the damage at the antenna is attributed to the primary shock.

A damage investigative and corrective action team issued a report.[1] That report contains a preliminary analysis of the subreflector-positioner assembly dynamic response to the earthquake. Since the report, a comprehensive finite-element model of the antenna structural system with subreflector, positioner, and concrete pedestal has been completed. The response derived from this model is contained herein. Small amounts of related coverage and material from the action team report[2] are reproduced here for convenient referral. The reference, however, covers more of the background, details, and proposed remedial actions.

Figure 2 contains schematics of the subreflector and positioner drive assembly, which were subject to major damage during the earthquake. Figure 3 shows six of the areas

[1] Engineering Analysis and Corrective Action Team, *DSS-14 70-meter Antenna Earthquake Damage Investigation*, vols. 1 and 2, JPL Report 890-251 (internal document), Jet Propulsion Laboratory, Pasadena, California, September 25, 1992.

[2] Ibid.

Z-axis actuator U-joints failed and have been circled in the figure. Another circle has been placed at the X-axis drive to indicate that the supporting bracket was bent. The X-axis actuator shaft was also bent, and four of the six safety cables failed when the actuator failures allowed the subreflector to drop. The axes denoted in these two figures are local axes fixed on the antenna: the Z-axis is the antenna-pointing axis, the X-axis is parallel to the elevation axis, and the Y-axis is vertical (positive upwards) when the antenna points to the horizon. At the 15-deg elevation angle, in effect at the time of the earthquake, the Y-axis actuators support almost all of the static weight of the positioner and the subreflector.

The subreflector impacted against a quadripod leg, which caused some damage to the subreflector and the leg. The subreflector was eventually wedged against the quadripod leg and supported by one of the intact safety cables, and possibly by the remaining Z-axis actuator and the damaged X-axis actuator. A failure scenario assembled in the action team report[3] assigns the first failure to the left side (as oriented in Fig. 3) Y-axis U-joint; the next failure (attributed to effects of transference of gravity loading and a rotation) was at a remaining Y-axis actuator U-joint. Then, it was proposed, the top (Fig. 3) Z-axis actuator U-joint failed, and this was followed by the impact of the falling torus on the X-actuator bracket. After this, the scenario continues to explain further events and observations of additional damage.

The original design called for identical Y- and Z-axis U-joints and a lower capacity design for the X-axis U-joints. The four intact Z-axis U-joints, one Y-axis U-joint, and both X-axis U-joints were returned to the laboratory for failure load tests. The failure loads for the five Z- or Y-axis U-joints were in the range of from 34,350 to 42,290 lb in tension, with a mean of 38,538 and standard deviation of 3,320 lb. The catalog value of the tension-rated load for these U-joints was 54,000 lb, and they were supposedly capable of withstanding temporary loads of 150 percent of the rated load. Therefore, it is evident that these U-joints were substandard. One X-axis U-joint failed in tension at 30,800 lb, and the other failed at 48,830 lb in compression. The foregoing values are all based upon the U-joints that survived the earthquake. Hence it could be concluded that in the field, the U-joints failed from the earthquake at loads less than those of the tests.

II. Ground Motion Time History Records

A California Institute of Technology Seismological Laboratory instrumentation station provided three-axis accelerograph records of the ground motion in the north–south, east–west, and vertical directions at the Echo Site, which is about 6 kilometers to the south of the Mars antenna. These records are plotted in Figs. 4(a), (b), and (c). Another set of tri-axial accelerograph records was also obtained at an intermediate-level platform of the Mars antenna instrument tower, which is shown in Fig. 5. Records are available for 40-sec durations at both locations and are digitized at the rates of 100 per sec for the Echo site and 200 per sec for the Mars site.

The maximum accelerations recorded at Echo were 4.8 percent of gravity (0.048 g) for the north–south component, 0.058 g for the east–west component, and 0.041 g for the vertical component. These are not large accelerations in comparison with those of past damage-producing earthquakes. However, the portions of the records showing the strongest motion are of long enough duration to be damaging.

The maximum accelerations recorded at the instrument tower platform were 0.20 g in a "longitudinal" direction, 0.16 g in a "transverse" (lateral) direction, and 0.16 g in the vertical direction. These records provide the responses at the platform, which in fact represent some amplification of the actual earthquake ground motion. Had the records been available for the site ground motion, rather than for the response to the ground motion, they would have served as the input for the analytical dynamics investigation of the earthquake response of the antenna.

III. Adjustments of Ground Motion Records

The Echo records would be an obvious choice for estimating the ground motion at the Mars antenna site, provided that the 6 kilometers of intervening strata to the Mars site were homogenous and not subject to discontinuities in physical properties. To test this, an analytical model of the instrument tower structure was assembled and subjected to the excitation defined by the Echo records. The purpose was to compare the output of the model derived at the platform level with the available records of tower response to the earthquake.

The analytical model was developed from a preliminary 12 degrees-of-freedom representation that was later adjusted to improve the agreement with field modal tests [1]. Since the tower appeared to be essentially symmetrical with respect to any two orthogonal vertical planes, a single two-dimensional model (height dimensions and horizontal displacements) was estimated to be adequate for vibratory motions parallel to the ground. The field testing program excited and measured the tower vibrations in the longitudinal and lateral directions. A separate one-dimensional

[3] Ibid.

model (height dimensions and vertical displacements) was developed for vertical vibration modes, but it was not possible to excite vertical mode vibrations in the field to check or adjust this model. The lowest frequencies (more than 15 Hz) computed from the vertical vibration model appear to be much higher than typical important excitation frequencies of earthquake ground motions.

Figure 6 contains comparisons of frequencies and mode shapes for the first three vibration modes from measurement and from the adjusted model. The frequencies are in agreement, as are the first two mode shapes. The third mode shapes differ, but this is not important because the frequency is above the range of significant earthquake excitation. There is a small lack of symmetry in the as-built tower with respect to the longitudinal and lateral directions. Consequently, the measured frequencies are slightly different for these two directions, and the tabulations in the figure show the ranges.

The recorded Echo north (north–south) and east (east–west) acceleration records were integrated to provide the associated ground displacements, which were then used as input to the model. Differences in the power spectral densities (PSD) of the computed acceleration responses were evident at the 3.5- and 10-Hz first- and second-mode natural frequencies when the spectral densities were compared with the PSD obtained from the direct Mars-site measurement records. The Echo acceleration records were then adjusted to reduce these differences by supplementing them with linear combinations of trial acceleration vectors. The combining factors were determined by a nonlinear least squares optimization to minimize the differences in the 1-Hz to 12-Hz frequency range between the PSD computed from the tower model and the PSD determined from the direct measurements. Figures 7(a) and 8(a) show the PSD curves obtained from the direct measurements and the curves obtained by calculations that used the original Echo ground motions as input. Figures 7(b) and 8(b) show improved agreement of the measurements with the calculations obtained by using the adjusted Echo records as inputs to the tower model. Figures 9 and 10 show the power spectra for the original and adjusted Echo ground accelerations. It can be seen that the adjustments provided only moderate changes to the original Echo data. The assumptions made in processing all of the foregoing data were (1) the ground motions could be assumed to be approximately stationary during the 15-sec to 26-sec time interval (11-sec) of the record, during which time all the motion records were judged to be the most intense, and (2) the effective damping ratio for the tower was 2 percent.

IV. Finite-Element Model

The finite-element method (FEM) design model for the antenna-tipping structure was developed in the mid-1980's. It contained 5500 degrees of freedom and represented one-half of the full structure. More recently, this model was extended to include the full structure, and the original set of three translational degrees of freedom at each node was supplemented by three more rotational degrees of freedom. This model, which now contains 38,000 degrees of freedom, runs on the NASTRAN structural analysis computer program and requires a Cray computer to accommodate the problem size readily and to provide a reasonable turnaround time. This model includes a representation of the subreflector-positioner component with 2500 degrees of freedom and a concrete pedestal component with an additional 11,000 degrees of freedom. These latter two components were successfully incorporated within the primary structure model after the publication of the action team report.[4]

Figure 11 represents a side view of the complete antenna model at the 15-deg earthquake incidence elevation. There are about 8000 nodes and 17,000 elements (13,000 bar elements, 2000 plate elements, and 2000 solid elements) in this model. Figure 12 shows a close-up of the quadripod apex, subreflector-positioner, and subreflector regions of the model. The tilt of the subreflector relative to the apex is standard because of the tri-cone configuration. Figure 13 shows a side-view cross-section of the pedestal component model, which consists entirely of solid elements.

V. Dynamic Analysis

The finite-element model problem (38,000 degrees of freedom) was processed by the NASTRAN structural analysis program on the Cray computer. The NASTRAN processing consisted only of solving the eigenvalue problem for natural frequencies and mode shapes for the 40 lowest modes. The NASTRAN output was post-processed by a FORTRAN program written to compute the elastic-rigid coupling matrix and effective modal weights according to algorithms provided in [2]. Selected components of the eigenvectors and modal forces in the actuator members were also extracted. All of the post-processed data were written in ASCII files and transferred to a 386 PC, where the dynamic response analysis to the earthquake was readily developed.

Conventional modal superposition analysis was used to generate response time histories of actuator forces and a

[4] Ibid.

subset of displacements at nodes to which the actuators were connected. The physical system was described by the generalized modal masses, elastic-rigid coupling matrices, and natural frequencies. The excitation to the system was provided by the Echo three-axis ground acceleration time histories as described above.

Two sets of ground motion time histories were processed; one set contained the original recorded Echo motions, and the other was the adjusted Echo motions. The model had been rotated about the elevation axis to the 15-deg elevation of the earthquake incident, so that the vertical earthquake records were applied along the model Z-axis. The antenna azimuth at earthquake incidence was 67 deg clockwise from north. Therefore, to invoke a consistent assumption, the Echo north–south and east–west data were rotated about a vertical axis to be aligned with the antenna model's north and east axes. Table 1 summarizes the maximum and minimum ground accelerations that were input to the models in the direction of the antenna axes after rotation.

VI. Computed Dynamic Actuator Forces

Three major assumptions in the computations were

(1) A power failure at the start of the earthquake caused an automatic application of the antenna brakes. The dynamic effects on the structure were assumed to be sufficiently attenuated at the time of the stronger ground motions to be ignored in the analysis.

(2) The damping ratio for all modes was 1 percent. This is based upon preliminary field measurements, during which the system was subjected to a sudden imposition of the brakes.

(3) All components remained intact during the linear-response analysis. Consequently, this assumption implies that the analysis can be meaningful only up to the time of the first component failure or yielding.

Figures 14 (a) through (f) show the dynamic force histories for the six actuators, based upon analysis of the full model with the adjusted Echo ground motions as the input excitations. The static weight loadings at the 15-deg elevation of −670, −589, 7460, 0, 11,750, and 11,420 lb have been included in the figure. Table 2 contains a summary of calculated dynamic forces based upon the conditions used to develop Fig. 14 and also from several other cases.

VII. Computed Dynamic Displacements and Accelerations

A few selected displacement time histories are shown in Fig. 15. All of these are in relative coordinates with respect to the ground motions. The total displacements are the sum of the relative displacements and the ground motion displacements. Although displacements in Figs. 15(a) and (b) are at the outboard ends of the actuators, the displacements at the inboard ends differ by only small percentages. The apex displacements in Figs. 15(c), (d), and (e) were obtained by averaging the displacements for a pair of nodes to each side of the center of the apex. The peak displacements of the X-axis actuator are about 50 percent greater than for the peak X-axis displacements of the apex. This could be because there is only a single X-axis actuator, which is supported by a relatively flexible bracket at its inboard end. On the other hand, the Y-axis actuator displacements are only slightly more than the apex Y-axis displacements.

The accelerations corresponding to the above relative displacements are shown in Fig. 16. To obtain the absolute accelerations, relative accelerations should be supplemented by adding the ground motion accelerations. Referring back to Table 1, it appears that the accelerations of the X-axis actuator indicate an amplification factor of about 25 with respect to the ground acceleration, and the Y-axis actuator amplification factors are about 17. The apex amplification factors are about 12, 16, and 6 in the X, Y, and Z directions, respectively.

VIII. Summary and Conclusions

The June 28 earthquake ground motion records at the Echo site were adjusted to provide output power spectra that were a close match to the power spectra of measured Mars site instrument tower records at a distance of 6 kilometers. A comprehensive finite-element method analytical model of the Mars antenna structural system was subjected to the excitation of the adjusted Echo ground motion. Dynamic analyses were completed to provide response time histories of forces and displacements associated with subreflector-positioner actuator components, some of which had failed during the earthquake.

The computed peak dynamic loads in the range of 30,000 to 35,000 lb for the two Y-axis actuators for which the U-joints had failed during the earthquake are consistently lower than laboratory failure load tests on surviving U-joints, which were in the range of 34,000 to 42,000 lb. The next largest forces from the analyses, of about 25,000 lb, were for the X-axis actuator. Nevertheless, this was still below the laboratory failure test load of 30,800 lb. Thus, it seems that the X-axis actuator could have survived undamaged from the earthquake except for the subsequent impact of the falling torus structure. In particular, these calculated maximum dynamic

the U-joints had failed during the earthquake are consistently lower than laboratory failure load tests on surviving U-joints, which were in the range of 34,000 to 42,000 lb. The next largest forces from the analyses, of about 25,000 lb, were for the X-axis actuator. Nevertheless, this was still below the laboratory failure test load of 30,800 lb. Thus, it seems that the X-axis actuator could have survived undamaged from the earthquake except for the subsequent impact of the falling torus structure. In particular, these calculated maximum dynamic forces are consistent with the failure scenario of the action team report.[5] All of the foregoing calculated results are sensitive to the structural damping. Here the damping ratio was assumed to be 1 percent based upon a limited amount of measured data.

Although the X-axis actuator could have survived the earthquake, the analysis for the acceleration amplification factors shows that the X-axis actuator is excessively flexible. The amplification factor for the X-axis actuator was about 25 times with respect to the input X-axis ground acceleration. This was about twice the amplification factor for the quadripod. The remaining Y- and Z-axis amplification factors for the quadripod were about 16 and 6, respectively. The Y-axis actuators, although deficient in load-carrying capacity, did not produce significantly different acceleration amplification factors from the quadripod apex.

The loads and displacement analyses here concentrated on the actuators and U-joints of the subreflector positioner. A separate and lengthier study would be needed to examine the effects of this earthquake on the complete structure. Nevertheless, it is possible that the examination here of the quadripod apex and subreflector positioner components may have considered the most vulnerable regions of the antenna. Future analysis of the seismic safety of the antenna would, of course, require an evaluation of the effects possible for a much broader range of seismic excitations than the single event considered here.

[5] Ibid.

Acknowledgments

JPL Engineering Analysis and Corrective Action (EACA) team members and contributors who provided background and evaluations are acknowledged specifically in the action team report[6] and its distribution list. We also wish to specifically recognize California Institute of Technology staff members who participated in the study—in particular, Professors J. Hall and W. Iwan for the suggestion that the Mars instrument tower response records be employed to particularize the site ground motion; Professor G. Housner, who proposed that the Echo ground motion could be used as a basis with supplemental adjustments to provide consistent tower response spectra; and Senior Research Fellow E. Hauksson, who provided the Echo ground motion records.

References

[1] *Experimental Modal Analysis of the DSS-14 Instrument Tower*, Report R9227-6405, AGBABIAN Associates, Pasadena, California, September 8, 1992.

[2] R. Levy, "Computation of Vibration Mode Elastic-Rigid and Effective Weight Coefficients from Finite-Element Computer Program Output," *The Telecommunications and Data Acquisition Progress Report 42-105*, vol. January–March 1991, Jet Propulsion Laboratory, Pasadena, California, pp. 13–20, May 15, 1991.

[6] Ibid.

Table 1. FEM ground accelerations after axis rotations.

Measurements		Accelerations, g		
		X-axis	Y-axis	Z-axis
Original Echo data	maximum	0.041	0.054	0.027
	minimum	−0.037	−0.053	−0.041
Adjusted Echo data	maximum	0.044	0.059	0.027
	minimum	−0.036	−0.058	−0.041

Table 2. Summary of extreme forces in the subreflector-positioner actuators.

Configuration	Actuator loads, kilo-pounds					
	Right-Z[a]	Left-Z[a]	Top-Z[a]	X	Left-Y	Right-Y
With adjusted Echo motion and pedestal:						
maximum	8.3	10.0	9.0	25.5	34.6	31.5
minimum	−8.6	−9.7	−11.3	−25.3	−12.7	−7.2
With original Echo motion and pedestal:						
maximum	7.5	9.3	8.9	23.7	32.8	30.4
minimum	−8.3	−9.2	−10.5	−23.6	−11.3	−6.3
With adjusted Echo motion but no pedestal:						
maximum	7.7	10.9	9.1	25.5	33.5	29.7
minimum	−6.7	−11.0	−11.0	−25.6	−11.5	−7.4
With original Echo motion and no pedestal:						
maximum	7.6	10.2	8.6	23.9	31.8	29.1
minimum	−6.7	−9.8	−10.1	−24.0	9.4	−6.0

[a] Does not include static weight loading at 15-deg elevation.

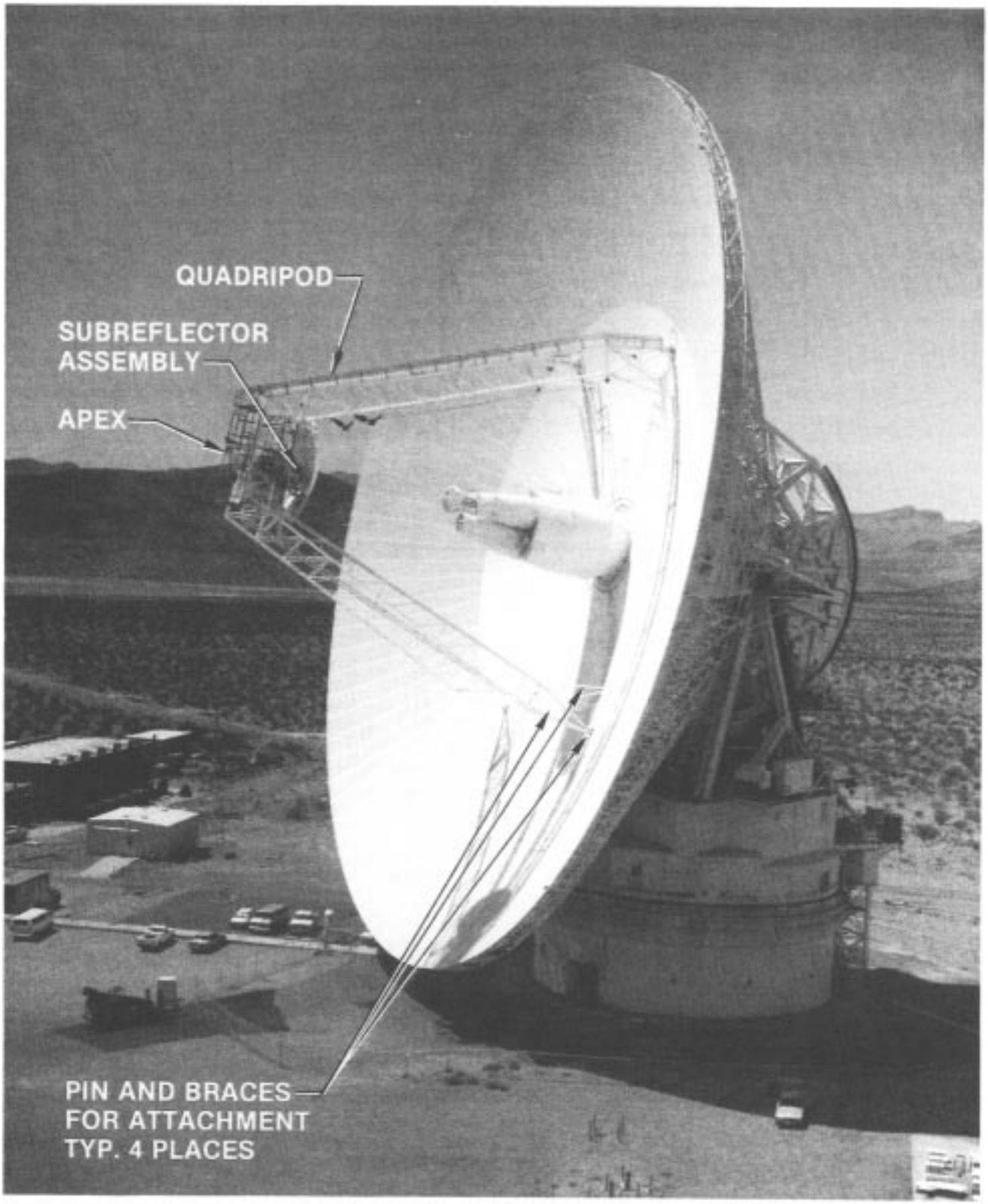

Fig. 1. DSS-14 (Mars) antenna at earthquake position.

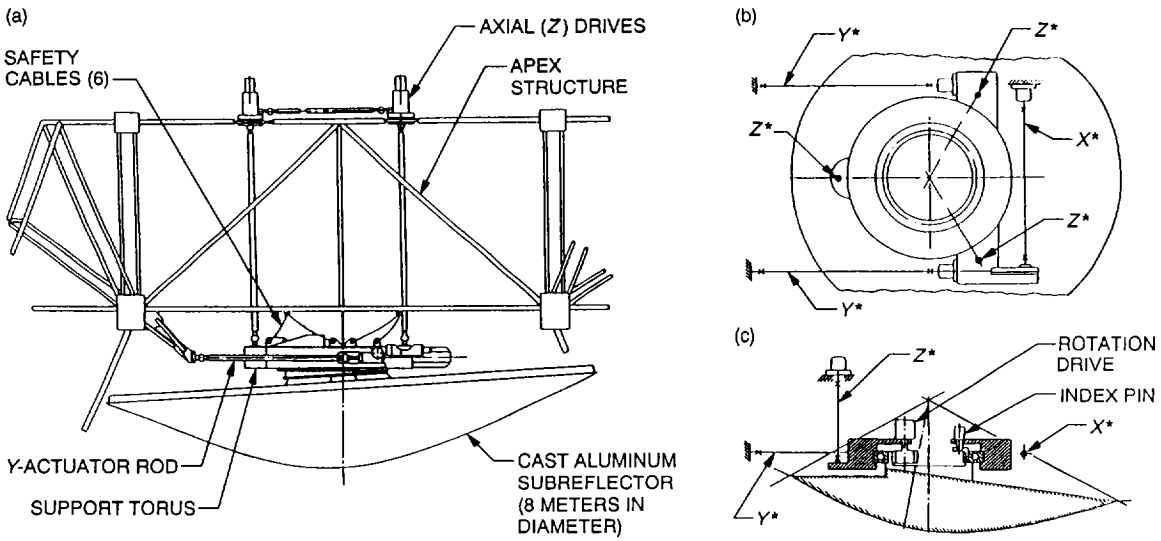

Fig. 2. Subreflector and positioner assembly: (a) elevation view, (b) plan view showing rotation bearing and actuator rods (with asterisks), and (c) elevation section showing rotation bearing and actuator rods (with asterisks).

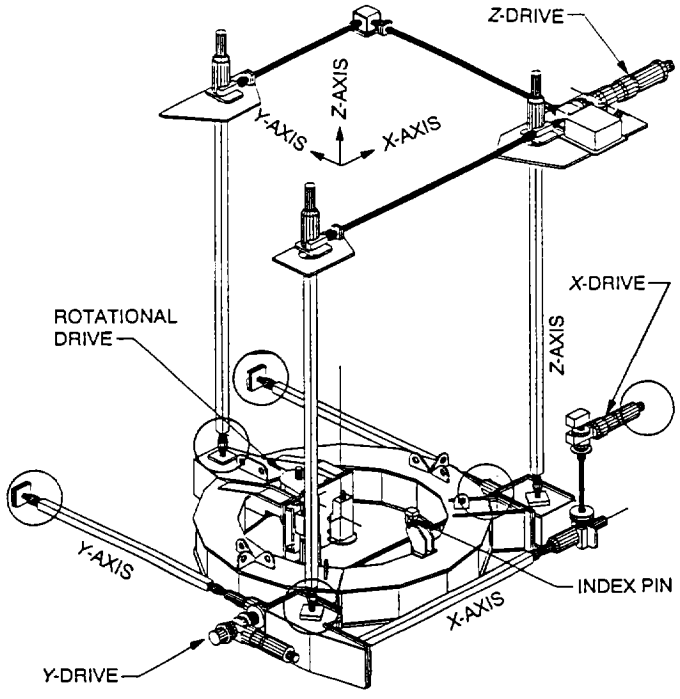

Fig. 3. Subreflector positioner damage points.

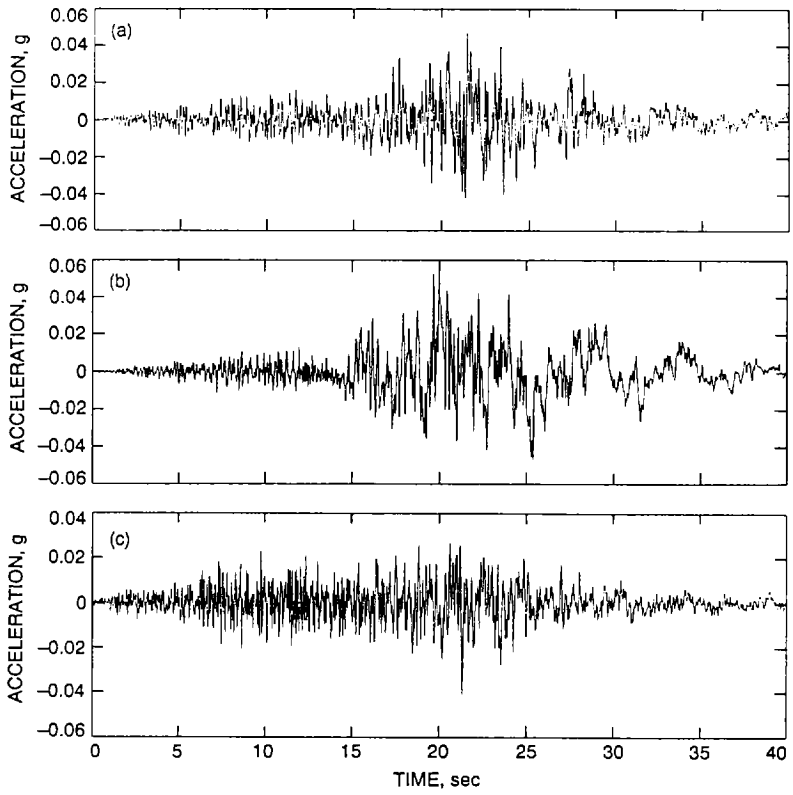

Fig. 4. Echo recorded ground motion for (a) north–south, (b) east–west, and (c) vertical.

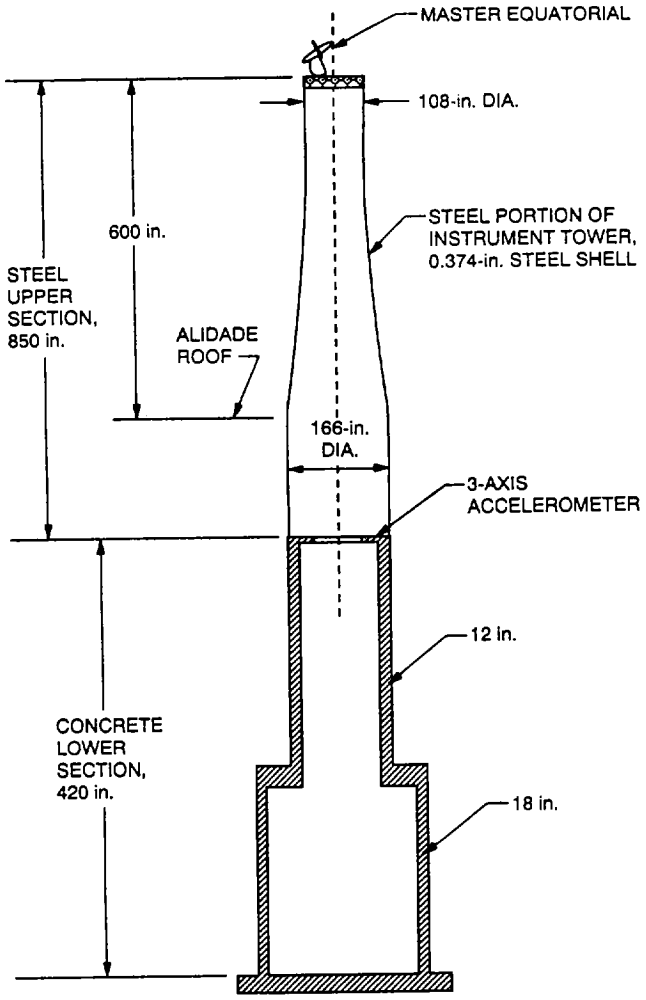

Fig. 5. Mars antenna instrument tower.

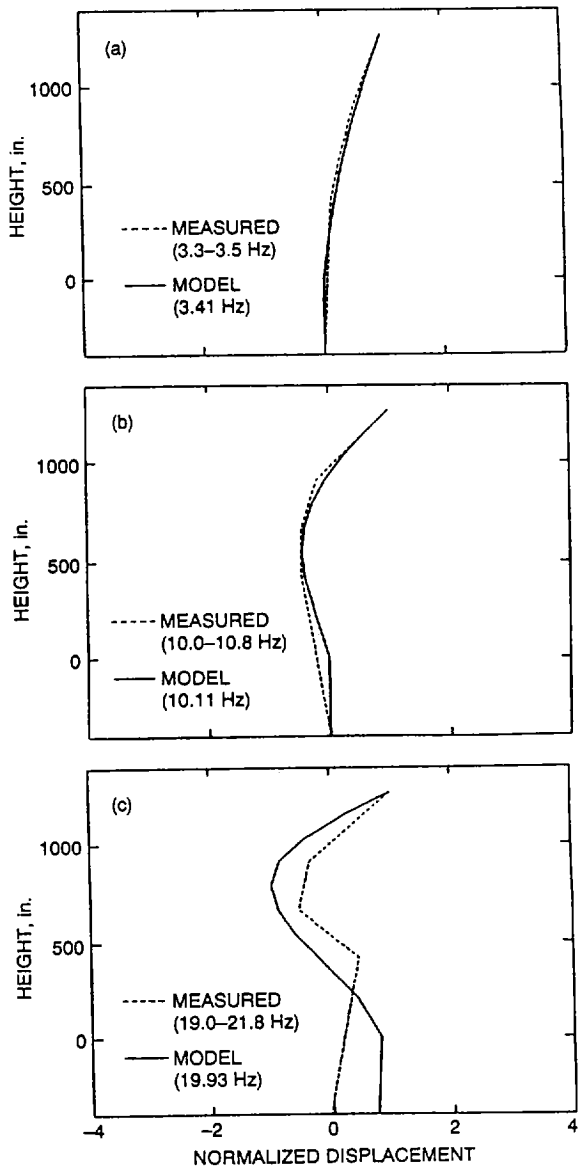

Fig. 6. Instrument tower measured and modeled vibration modes: (a) first mode, (b) second mode, and (c) third mode.

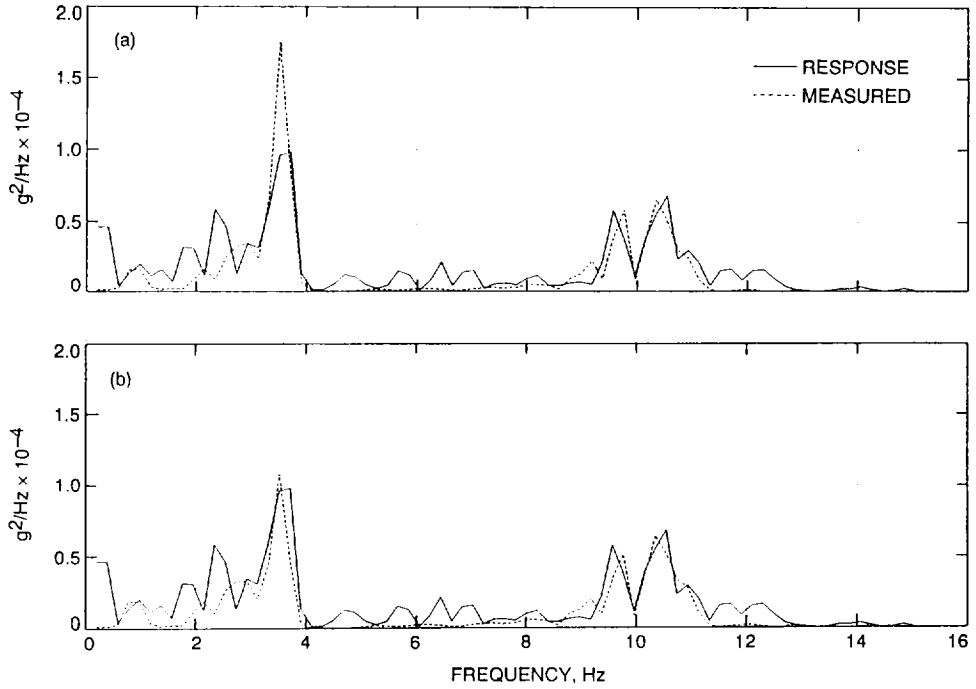

Fig. 7. Tower lateral response spectral densities: (a) original Echo north and (b) adjusted Echo north.

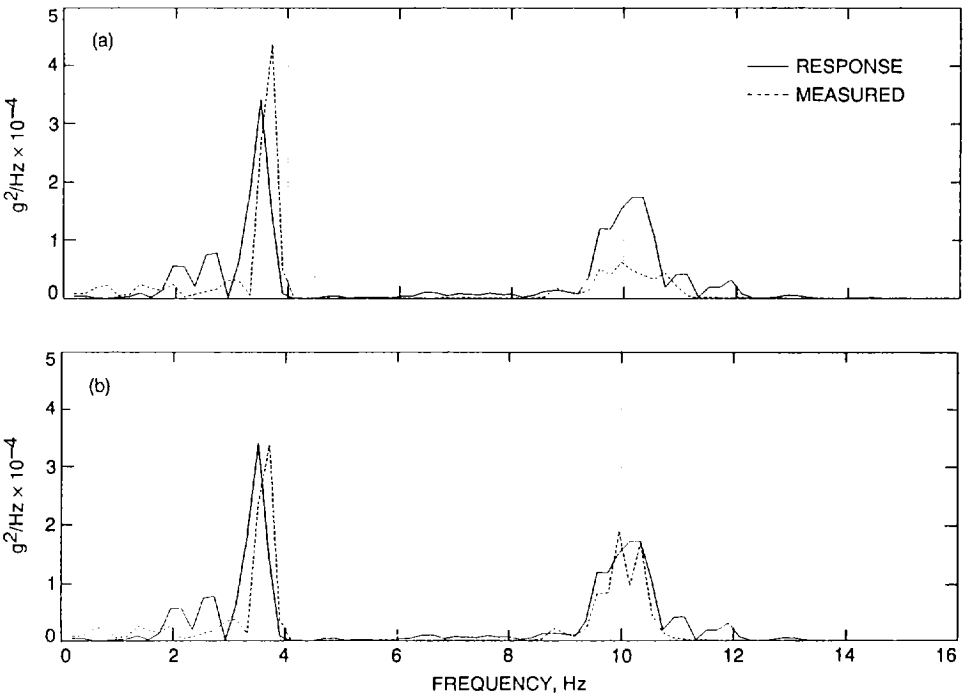

Fig. 8. Tower longitudinal response spectral densities: (a) original Echo east and (b) adjusted Echo east.

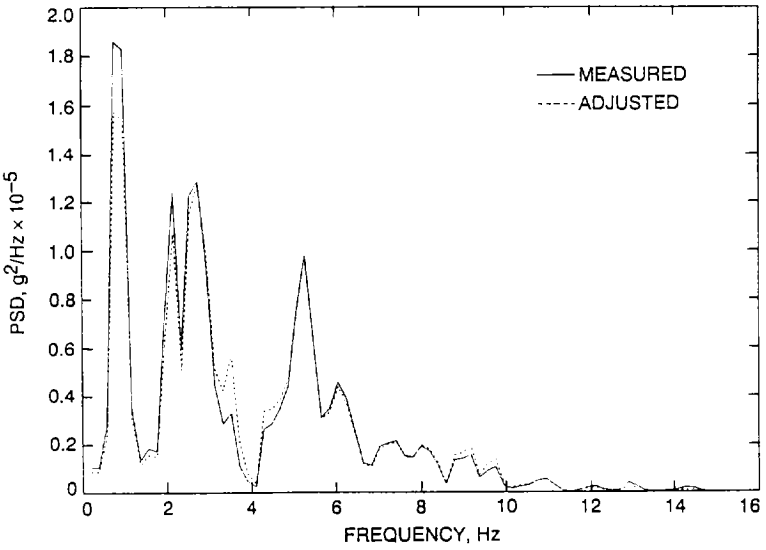

Fig. 9. Power spectra, Echo north record.

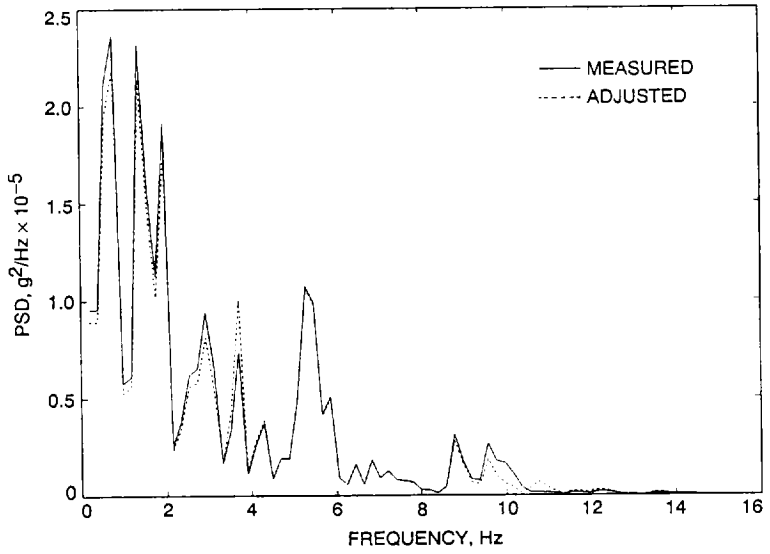

Fig. 10. Power spectra, Echo east record.

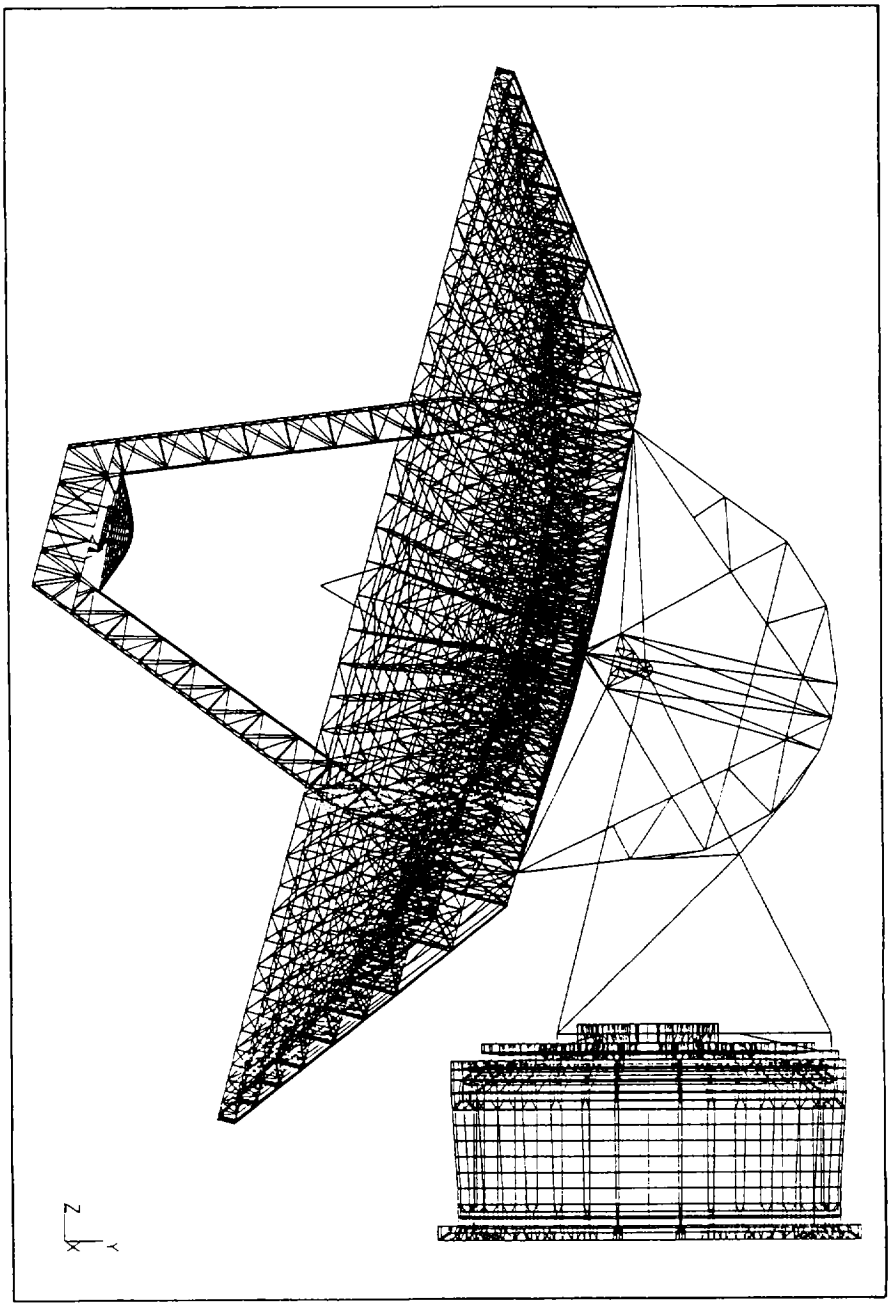

Fig. 11. Mars antenna finite-element model.

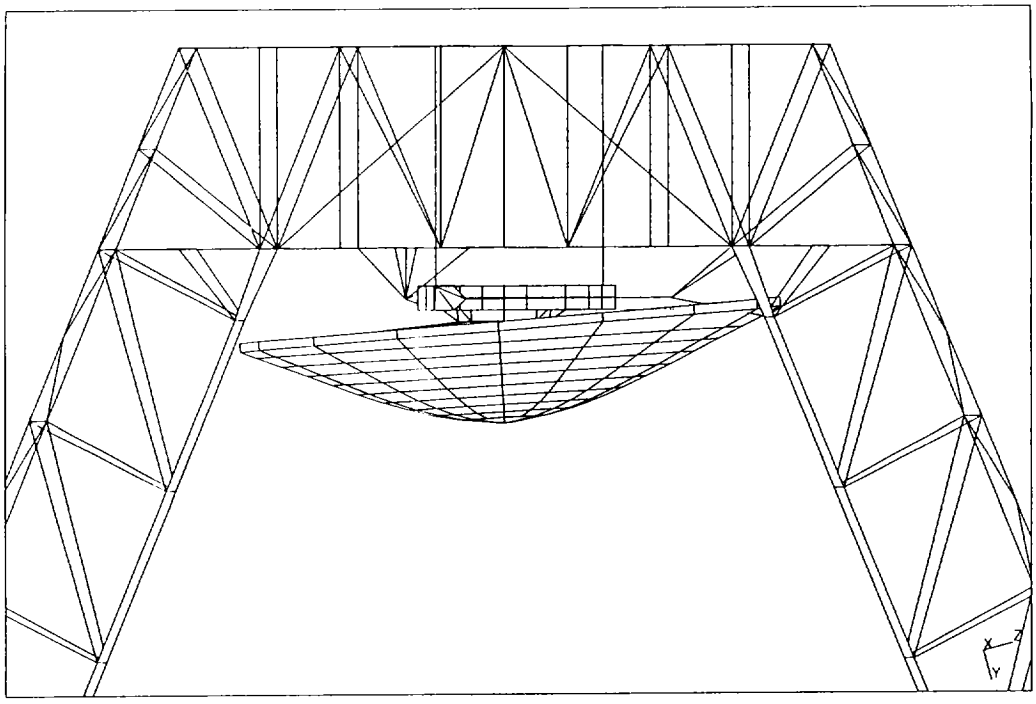

Fig. 12. Quadripod apex and subreflector components of the model.

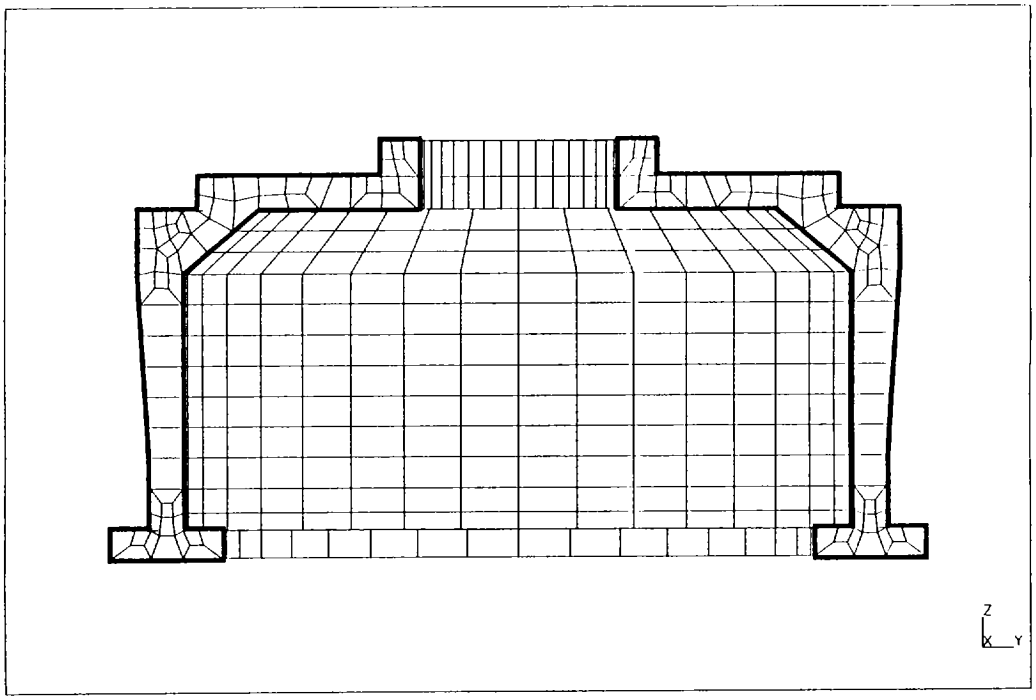

Fig. 13. Pedestal component of the model.

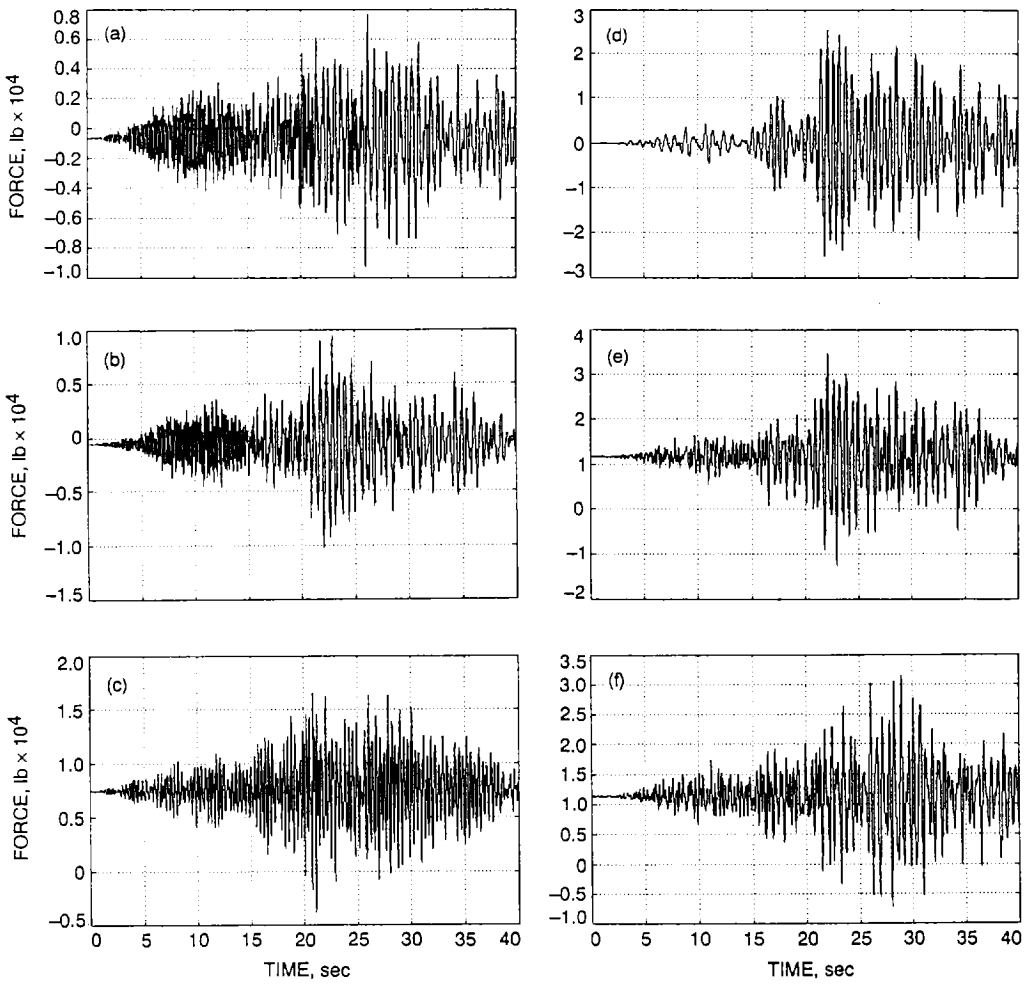

Fig. 14. Dynamic forces (a) on the right *Z*-actuator, (b) on the left *Z*-actuator, (c) on the top *Z*-actuator, (d) on the *X*-actuator, (e) on the left *Y*-actuator, and (f) on the right *Y*-actuator.

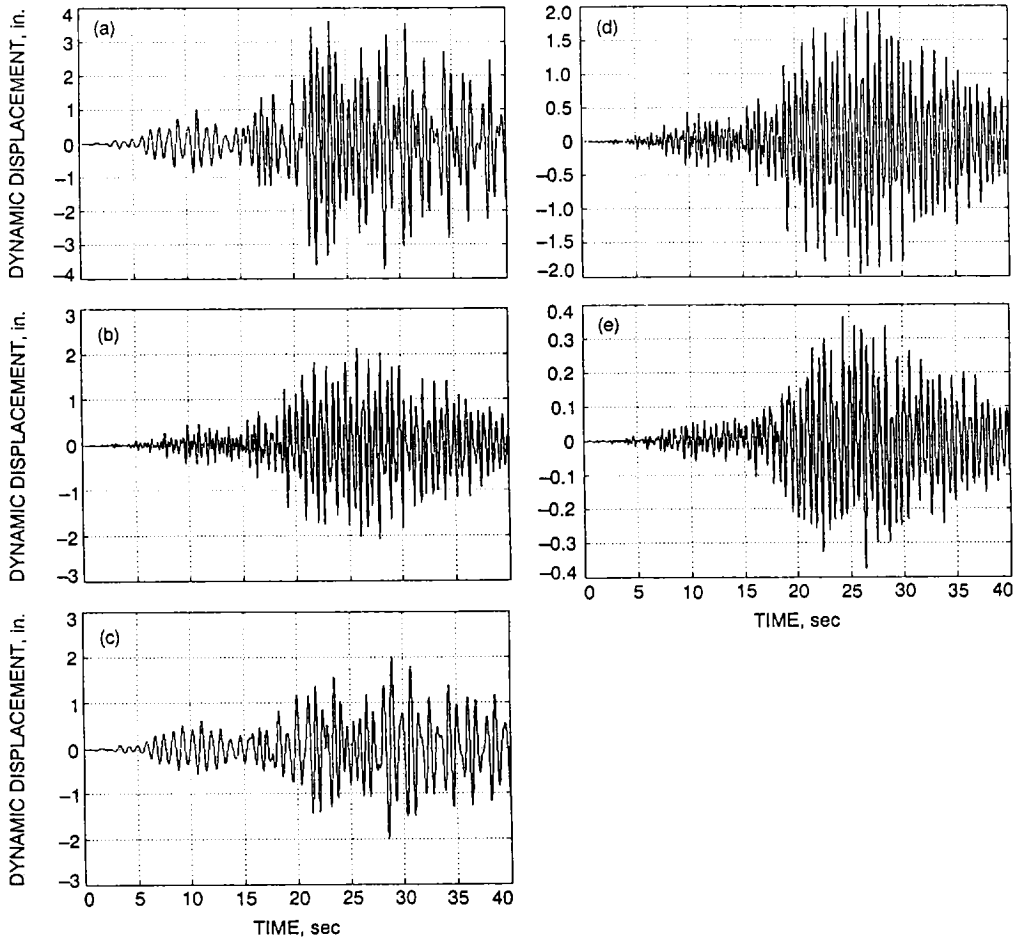

Fig. 15. Dynamic displacements: (a) outboard end—*X*-actuator, (b) left side of the outboard end—*Y*-actuator, (c) average apex—*X* direction, (d) average apex—*Y* direction, and (e) average apex—*Z* direction.

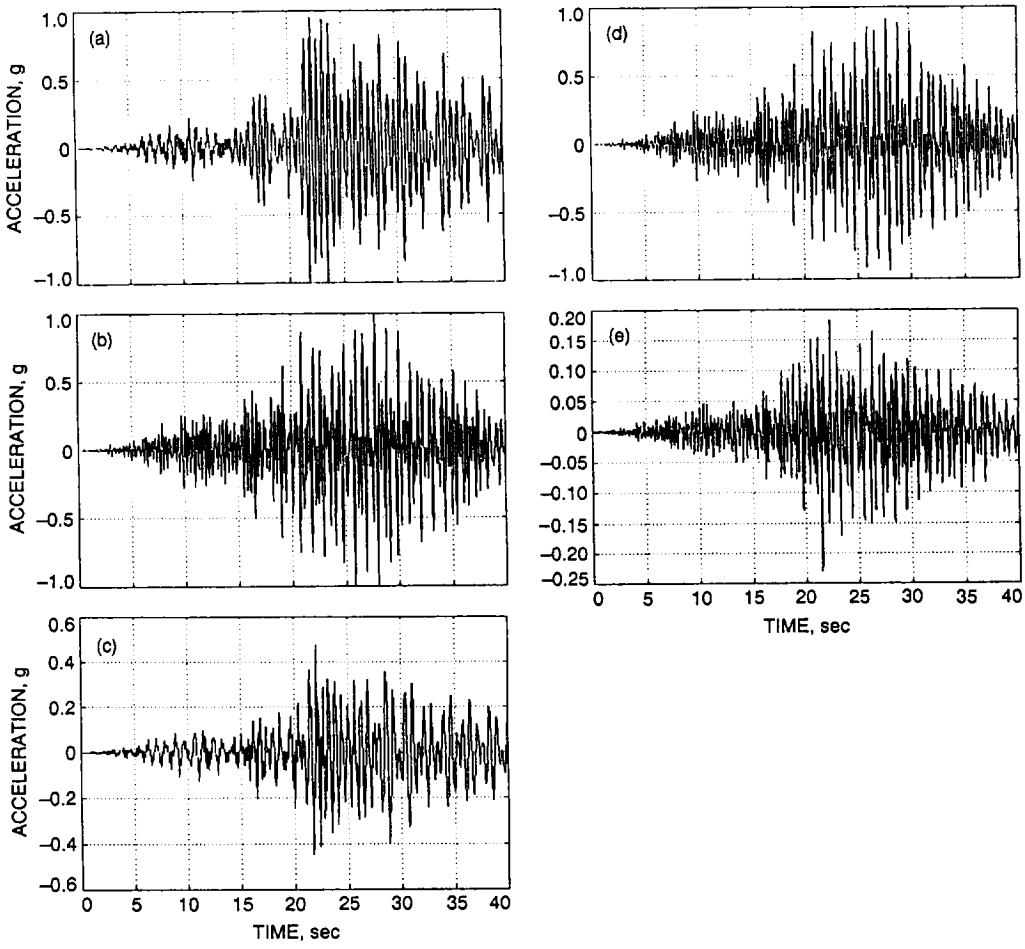

Fig. 16. Dynamic accelerations: (a) *X*-actuator, (b) left-side *Y*-actuator, (c) apex—*X* direction, (d) apex—*Y* direction, and (e) apex—*Z* direction.